First results of the polarimeter for the Large APEX Bolometer Camera (LABOCA)

Giorgio Siringo[a], Attila Kovács[c], Ernst Kreysa[b], Frederic Schuller[a], Axel Weiss[b], Rolf Guesten[b], Talayeh Hezareh[b], Karl M. Menten[b], Helmut Wiesemeyer[b], Michael Dumke[a], Francisco Montenegro[a], Rodrigo Parra[a]

[a]European Southern Observatory, Av. Alonso de Cordova 3107, Santiago, Chile;
[b]Max-Planck-Institut für Radioastronomie, Auf dem Hügel 69, 53121 Bonn, Germany;
[c]University of Minnesota, 116 Church St SE, Minneapolis, MN 55414, USA;

ABSTRACT

An enhanced version of the "Polarimeter für bolometer Kameras" (PolKa) has been installed on the APEX telescope (Atacama Pathfinder EXperiment) in October 2009, to work in combination with LABOCA (the Large APEX Bolometer Camera). This polarimeter was included in the design of LABOCA's optics from the beginning and it is now going through a commissioning and science verification phase. The combination of PolKa, LABOCA and APEX provides superior capabilities in mapping the polarization of the continuum at submillimeter wavelengths. We present here some preliminary results of the last commissioning run.

Keywords: submillimeter, polarization, bolometer, array, APEX, LABOCA

1. INTRODUCTION

Submillimeter continuum radiation can be partially linearly polarized. The processes that produce measurable levels of linear polarization can have different nature and depend on the type of astrophysical source that is considered.

Optically thin synchrotron emission from extragalactic objects, like radio galaxies and active galactic nuclei, is intrinsically linearly polarized. The degree of polarization depends on the strength of the magnetic field but also on the morphology of the source and on its orientation along the line of sight (see Cawthorne et al. 1993[[1]]).

Interstellar molecular clouds, in our Galaxy or in other galaxies, can be sources of linearly polarized continuum emission. In this case the polarization is produced by partial magnetic alignment of elongated dust grains (Hildebrand 1988[[2]]).

In both cases, the morphology of the magnetic field can be deduced from the direction of the polarization vectors, and polarimetry at millimeter and submillimeter wavelengths can trace the magnetic field in a more direct way than in the optical and radio regimes, where scattering and Faraday rotation can dominate the polarized signals. In the latter case, the emission is almost always optically thin, thus bolometers are the ideal detectors because the bolometric signal is proportional to the dust column density. Practically speaking, this makes dense cloud portions, in particular those associated with star-forming regions and protostellar envelopes, promising targets for polarimetry using bolometers.

The last decades saw an increasing effort in the development of receivers for continuum emission at millimeter and submillimeter wavelengths. The biggest step forward has been the introduction of bolometer arrays, devices made of several bolometers joint together in a larger structure (the array) where they perform simultaneous multi-beam observations.

The Large APEX Bolometer Camera (LABOCA, Siringo et al. 2009[[3]]) with its field of view of more than 100 squared arc-minutes is one of the largest submillimeter bolometer camera available today. LABOCA is a bolometer camera specifically designed for fast mapping of large sky areas at relatively high resolution and

Further author information: (Send correspondence to G.Siringo)
e-mail: gsiringo@eso.org web: http://www.eso.org

sensitivity. It was developed by the bolometer group of the Millimeter and Submillimeter Astronomy Group at the Max-Planck-Institut für Radioastronomie of Bonn (MPIfR) and commissioned in May 2007 as facility instrument on the Atacama Pathfinder Experiment telescope (APEX, Güsten et al. 2006[4]), a collaborative effort between MPIfR, the European Southern Observatory (ESO) and the Onsala Space Observatory (OSO).

APEX, as the name implies, serves as a pathfinder for the exploration of the submillimeter sky, in particular by performing large angular scale observations for later Atacama Large Millimeter Array (ALMA) follow-up studies on selected regions at much smaller angular scale.

The bolometer group of Bonn has developed a polarimeter that works in combination with LABOCA at APEX. We present here a description of this instrument and some preliminary results.

2. INSTRUMENT OVERVIEW

The polarimeter for LABOCA is an enhanced version of the polarimeter for bolometer cameras that was developed at MPIfR between 2000 and 2004. The design of this instrument (named *PolKa* after the German *Polarimeter für Bolometer Kameras*) was aimed to provide a versatile instrument, capable of giving good results with any of the MPIfR bolometer arrays, at different wavelengths and on different telescopes. A complete description and some results are presented in G. Siringo 2003[5] and Siringo et al. 2004[6].

2.1 Principle of operation

In order to extract the polarized component from the unpolarized signal and foregrounds it is common to use a polarization modulator to modulate the polarized component of the incoming radiation at a precise frequency. If the modulation acts only on the Q and U Stokes parameters of the radiation, the total intensity I will be unchanged, at least in the ideal case.

Since MPIfR bolometers are only sensitive to the total intensity I of the wave, a linear polarizer must be inserted along the optical path to transduce the modulation of Stokes Q and U into a modulation of I. PolKa uses a rotating half-wave plate (HWP) as polarization modulator and free-standing wire-grids as linear polarizers.

2.2 Continuous spinning technique and Stokes parameters

Placing a rotating HWP in the beam path will produce a modulation of the Stokes parameters, but the total intensity will remain unchanged. To quantify this assertion, let us consider the Müller matrix for an HWP rotating at angular velocity ω[7].

$$\mathbf{H}(\omega t) = \begin{pmatrix} 1 & 0 & 0 & 0 \\ 0 & \cos 4\omega t & \sin 4\omega t & 0 \\ 0 & \sin 4\omega t & -\cos 4\omega t & 0 \\ 0 & 0 & 0 & -1 \end{pmatrix} \tag{1}$$

If we compare this matrix to a rotation matrix, we see that it produces a rotation of the polarization vector in the direction opposite to the mechanical rotation of the device. More importantly, we see that the rotation frequency of the polarization vector is doubled: this is the biggest benefit that we gain by using an HWP instead of a rotating linear polarizer. Most of the spurious effects, in fact, will have a frequency equal to the mechanical one, ω, while the polarization signal will be modulated at 4ω resulting in an improved extraction of the signal from foreground and systematic effects. The Stokes vector modulated by the HWP is

$$\mathbf{H}(\omega t) \begin{pmatrix} I \\ Q \\ U \\ V \end{pmatrix} = \begin{pmatrix} I \\ Q\cos 4\omega t + U \sin 4\omega t \\ Q \sin 4\omega t - U\cos 4\omega t \\ -V \end{pmatrix} \tag{2}$$

and we see that, in the ideal case, the total intensity I of the incoming radiation is not modified because the polarization vector is rotated without any change in its magnitude.

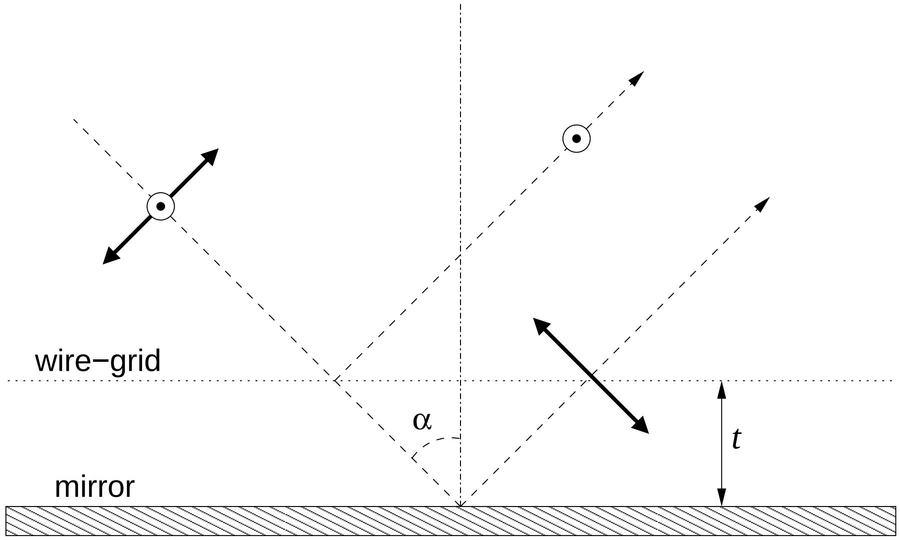

Figure 1. Scheme of a reflection-type half-wave plate. The incident radiation is divided into two beams with orthogonal polarization states. The two emerging rays will have a relative phase shift proportional to t.

At this point we introduce a fixed linear polarizer along the beam to produce an intensity modulation detectable by the bolometers. The bolometer output is

$$V_{\mathrm{H}} = \frac{1}{2}\left(I + Q\cos 4\omega t + U\sin 4\omega t\right) \tag{3}$$

$$V_{\mathrm{V}} = \frac{1}{2}\left(I - Q\cos 4\omega t - U\sin 4\omega t\right), \tag{4}$$

in the cases of a horizontal and a vertical linear polarizer respectively. The Stokes parameters of the linear polarization can be then extracted by those signals using synchronous demodulation methods.

2.3 The Reflective Half-Wave Plate (RHWP)

The polarization modulator used in PolKa is a rotating reflection-type half-wave plate (hereafter RHWP). The RHWP mainly consists of two parts: a wire-grid linear polarizer and a plane mirror, kept parallel to each other. By tuning the distance t between the two parts (see Fig. 1), it is possible to produce a phase shift between the two components of polarization, because one is reflected by the wires and the other one by the mirror, causing a difference in path length. The phase shift is given by the simple relation

$$\varphi(\lambda) = 2\pi\frac{t}{\lambda\cos\alpha} \tag{5}$$

where t is the distance between the polarizer and the mirror, α is the angle of incidence of the incoming radiation and λ is the operating wavelength. To have an HWP we assign $\varphi = \pi$ and the value of t for a central operating wavelength λ_0 is given by

$$t = \frac{1}{2}\lambda_0\cos\alpha \tag{6}$$

The RHWP works with reflections: even small oscillations of the rotation axis could produce large oscillations of the beam, increasing the noise of the measurements. On the other hand, the RHWP has the advantage that radiation does not pass through it and it can therefore be supported from the back. For these reasons we decided to mount it on a motorized air bearing. This device, which has an embedded on-axis electric motor, maintains the rotation plane within less than 1 μm. To minimize the errors in positioning the wire-grid parallel to the mirror, we reduced the number of surfaces to be machined with high accuracy to only two: the mirror plate and the upper side of the polarizer frame. The mirror plate is mounted on the air bearing and the distance of the wire-grid can be tuned to the operating wavelength (see Eq. (6)) by means of three micrometer heads.

Large wire-grid polarizers were produced at MPIfR purposely for the RHWP. These grids have a clear aperture of 246 mm with 20 μm tungsten wires and 63 μm grid step. The measured mean error in the wire spacing is 18 μm rms. Before the beginning of the observations the RHWP must be accurately tuned to maximize the polarization modulation efficiency.

It is worth noting that the RHWP is actually a tunable retarder that can be tuned to produce any phase shift: when tuned to produce a 90° phase shift, the same device can be used to modulate circular polarization.

3. PREVIOUS INSTALLATIONS

The PolKa polarimeter has been already installed on other two radio telescopes, before the actual installation on APEX.

3.1 At the Heinrich-Hertz Telescope (HHT) - 2001/2002

PolKa was tested at the Heinrich Hertz Telescope (hereafter HHT, also known as SMT[8]), a 10 meter submillimeter telescope (at 3200 m on Mt. Graham, AZ, USA) that was equipped with a 19-channel MPIfR bolometer array operating at 870 μm, today decommissioned. In May 2001 we made a first test with an undersized prototype of the RHWP. Unfortunately the weather didn't allow us to get any astronomical data, nevertheless the telescope run was useful to identify problems and to perform some calibrations. A second, more fruitful run with a full size RHWP was made in January 2002[5,6].

The receiver and its electronics, already existing at the telescope, were optimized to work at the frequency of the telescope's chopping secondary mirror (hereafter called wobbler), in most cases 2 Hz. For this reason, the amplifiers had high-pass filters cutting off signals below 1 Hz to suppress 1/f noise and very slow fluctuations of the signals. If we apply such a filter to Eqs. (3) and (4) we see that the information about the total intensity of the signal is lost because it is not modulated. Observations were therefore done alternating between two modes:first a photometric observation was done to detect the total flux of the source, using the wobbler to modulate Stokes I; then a polarization observation, done without using the wobbler but modulating Stokes Q and U with the polarimeter. To reduce the systematic effects and for a better removal of the spurious polarization, each polarization scan was made twice, once using an horizontal analyzer and once using a vertical one. We were forced to use two data acquisition systems, one for total intensity and one for polarization observations, and then merge the data offline. Moreover, given the temporary nature of the installation, no effort was devoted to make the system remotely controllable and the switch-over between polarization and photometry required manual intervention to exchange the analyzers and to switch on and off the modulator.

3.2 At the IRAM 30 m Millimeter Radio Telescope (MRT) - 2004

PolKa was shortly tested at the IRAM MRT[9] (Pico Veleta, Spain) in June 2004, working at the central wavelength of 1.2 mm in combination with the MAMBO-1 bolometer camera[10].

The weather didn't permit any science observations, however we could perform some technical tasks as calibrations and spurious polarization characterization. The polarimeter showed again high polarization efficiency and low systematics, proving the effective versatility of a polarimeter based on a tunable, reflection-type HWP. Moreover, this time we used a motorized filter exchanger, remotely controlled through the local network.

4. AT APEX

An enhanced version of the PolKa polarimeter was shipped from Bonn to APEX in 2008. Unfortunately the air bearing was damaged during the transport and it was sent back to Europe for repair. In the meanwhile, the installation of the other components was done in successive steps. The full system was ready at the end of October 2009. This installation, in contrast to the previous ones at the HHT and at the MRT, is permanent: the polarimeter is going to be available for use with LABOCA as long as this receiver is maintained in operation.

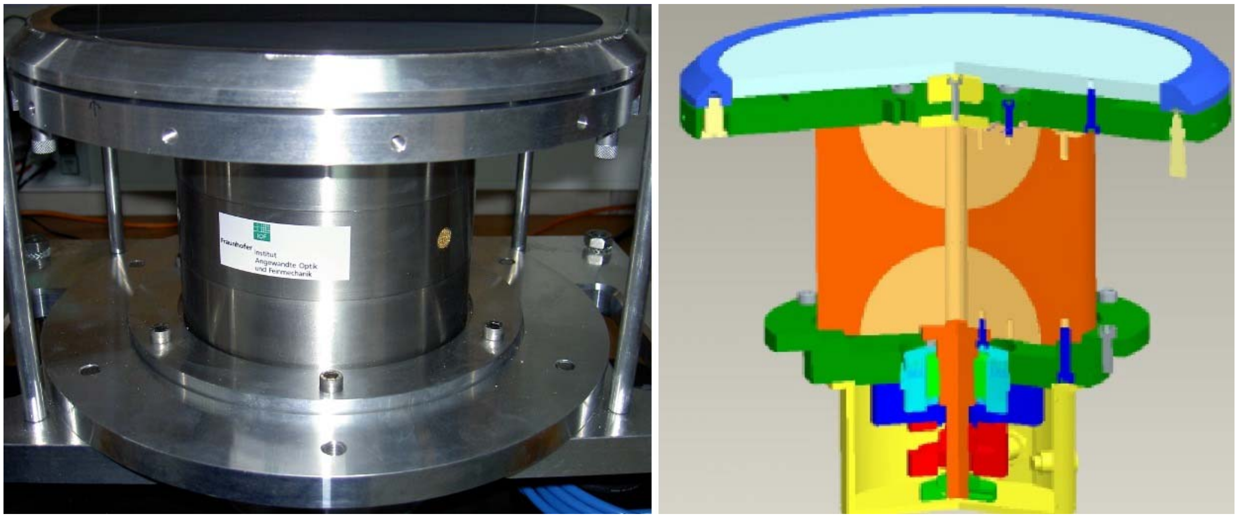

Figure 2. Left: a picture of the new RWHP module in a lab at APEX, before being installed in the receiver cabin. Right: a schematic drawing showing a section of the modulator. The two hemispheres represent the air bearing.

4.1 New polarization modulator

The polarimeter for LABOCA has a new modulator assembled by the Fraunhofer Institute for Applied Optics and Precision Engineering (IOF) of Jena, Germany (see Fig. 2).

The modulator is assembled on a motorized, double-sphere, rotary air bearing (DLL200, Mikromechanik GmbH). A metal mirror of optical quality (manufactured at IOF) is attached to the upper part of the rotor. The RWHP is composed with the same wire-grid polarizer used in the previous versions of PolKa, described in Sect. 2.3. Precision positioning of the polarizer in front of the mirror is ensured by three micrometeric screws. At the lower shaft of the rotor is connected one incremental encoder (Heidenhain ERO 1285 with IBV606 interpolator) that produces two trains of 2048 pulses in quadrature, per rotation. The position angle of the RHWP can thus be measured with an angular accuracy of $\sim 10'$. The air bearing requires a pressure of 5 bar, provided by a dedicated compressor. The unit is operated via a controller connected to the serial server of LABOCA and can be completely controlled remotely from the local network.

4.2 Filter wheel

As described in Sect. 2, between the modulator and the bolometers we need to insert a linear polarizer to transduce Stokes Q and U modulation into a measurable I modulation. From our experience at the HHT, we know that combining data acquired with orthogonal analyzers (horizontal and vertical in our description) can reduce the contribution of systematic effects on the final results of the data reduction. For this purpose we designed a filter wheel unit that holds two free-standing wire-grid polarizers (see Fig. 3). The wheel can be rotated to exchange the analyzer from orthogonal to vertical and vice-versa. Additionally, the unit can be rotated between other two positions: an empty slot, for total power observations, and a hot load, used for flux calibration.

The two polarizers are two identical wire-grids, produced at MPIfR, of 146 mm clear aperture, made of gold-coated tungsten wires with a diameter of 25 μm at a grid step of 100 μm. The wheel is moved by a step motor and can be remotely controlled.

4.3 Incorporation in the optics of LABOCA

LABOCA is located in the Cassegrain cabin of the APEX telescope and the optical coupling to the telescope is provided by a series of 5 metal mirrors and a lens (see Siringo et al. 2009[3] for the description of the optics.) The polarimeter was included in the design of the optics from the beginning, The polarization modulator has been incorporated simply by replacing one plane mirror (M6, see Fig.4) with the RHWP. The paddle used for the hot calibration was replaced by the filter wheel. No other modifications were required.

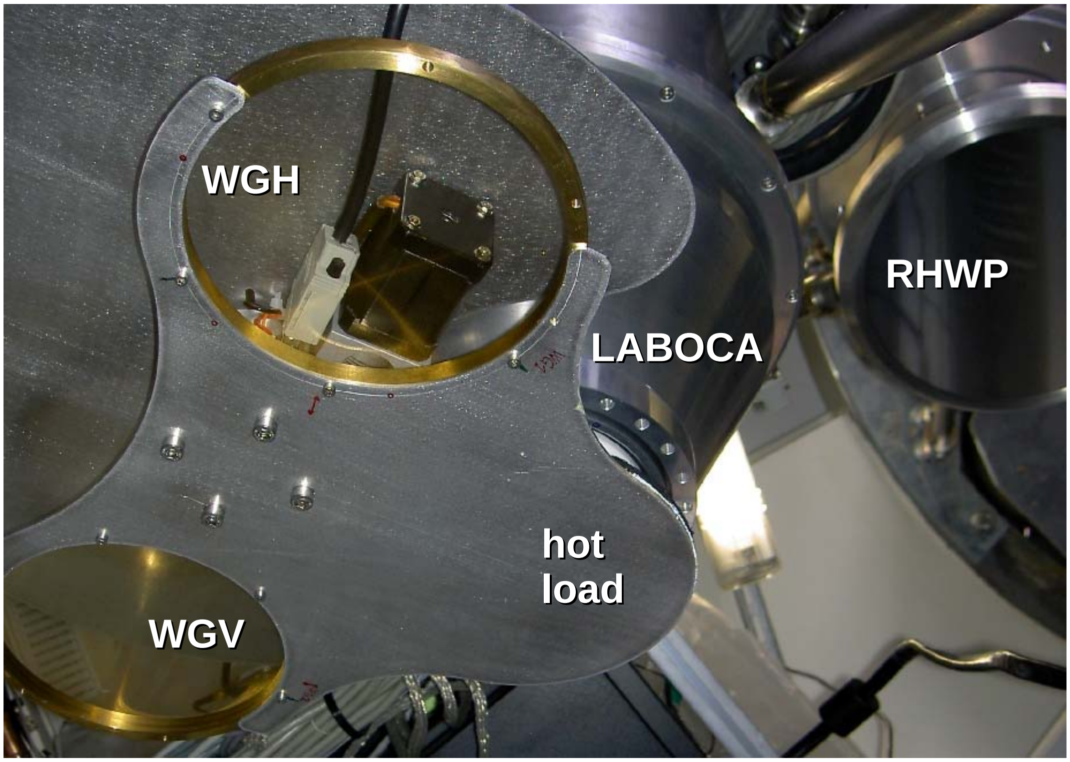

Figure 3. The picture shows the filter wheel attached at the lower part of LABOCA. The wheel is in the position for calibration on the hot load. The step motor used to move the wheel is visible through the WGH polarizer. The polarization modulator (RHWP) is also visible in the background.

At the position of M6, where the RWHP is today, the angle of incidence is only $\alpha = 16\overset{\circ}{.}23$ (see Fig. 1 and Eqs. 5 and 6.), while at the HHT and MRT it was 45°.

4.4 Observations

The polarimeter has the status of PI instrument on APEX, therefore it can be operated only during MPIfR observing time. This condition limits the observing time available for polarization observations. The hardware was installed on APEX at the end of October 2009, since then we only had three short observing periods. In all cases weather conditions were never too good, with a content of precipitable water vapor (PWV) in the range 1.5 mm - 2.5 mm that, at the wavelength of LABOCA (870 μm) corresponds to a zenith opacity of 0.5 - 0.7.

Before the beginning of the observations the RHWP is accurately tuned to maximize the polarization modulation efficiency. For that, a reference polarized target is placed at the focal plane of the telescope and the distance between the grid and the mirror is adjusted maximizing the modulated signals.

We use the same hardware and a slightly modified data acquisition chain to operate LABOCA. New software has been installed to operate the polarimeter and to acquire the position reference from the encoder embedded in the APEX Control Software[11].

The bolometers of LABOCA are DC-coupled and the total intensity is preserved in the acquired signals, as described by Eqs. (3) and (4), for observations done with horizontal and vertical analyzer respectively. There is an advantage here in comparison to the previous installations of PolKa: in fact, we get simultaneously Stokes I, Q, U and there is no need to repeat the observation in total power, as it was required at the HHT and at the MRT (see Sect. 3.1).

In November 2009 there was a first, preliminary test of the hardware with a few hours on sky. The tests confirmed the validity of the peculiar design concept of this instrument, besides showing the limitations of hardware and software at that time. In April 2011 the polarimeter was tested again on sky, with only minor

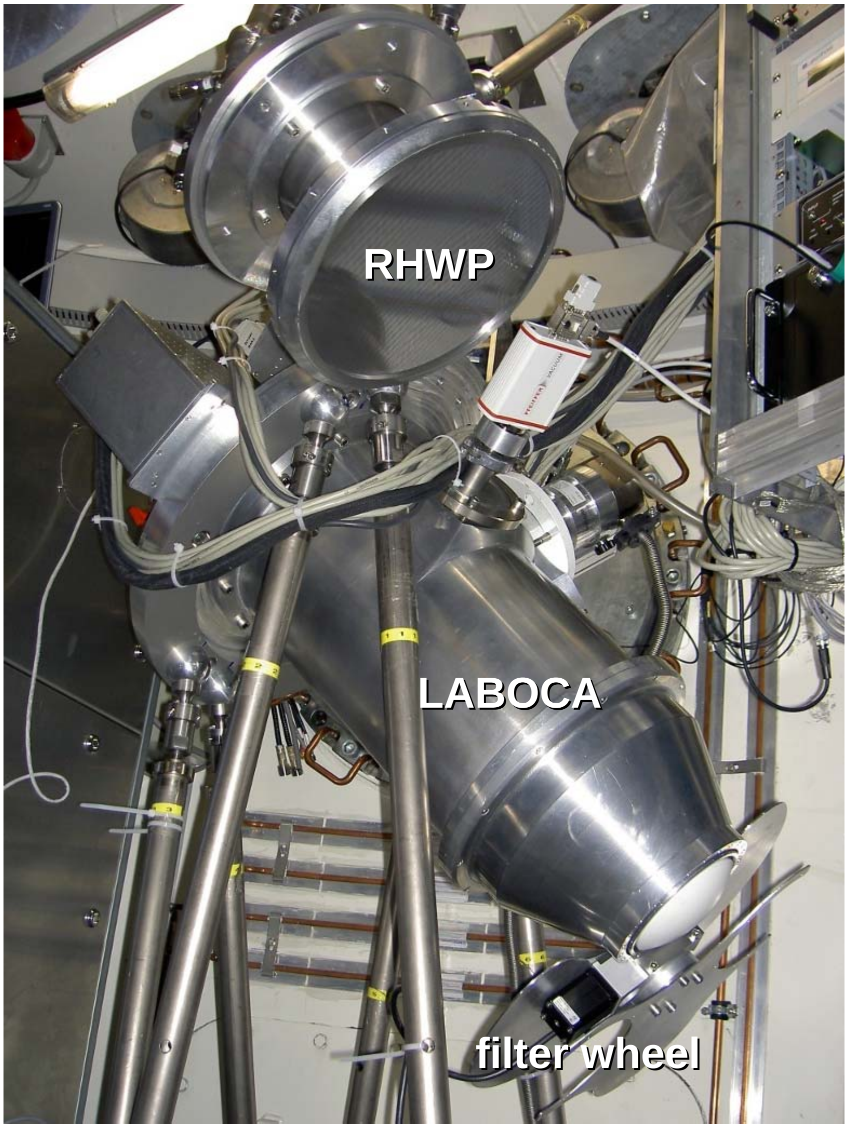

Figure 4. A picture of the polarimeter installed in the Cassegrain receiver cabin of APEX. The polarization modulator is the round object visible in the upper part of the picture. In the center, the cryostat of LABOCA with the filter wheel mounted at the lowest extremity. See also Figg. 3 and 4 in Siringo et al. 2009[3].

changes to the configuration of the hardware and software. The last commissioning run was spanning almost two weeks during the first half of December 2011. Some technical issues mainly related to data acquisition have been identified and partially fixed.

4.5 Observing Modes

We defined two main observing modes, one for mapping of extended sources and one for unresolved sources (a.k.a. point sources).

4.5.1 Mapping

Observations are done using a compact raster of spiral patterns, similar to the mapping mode typically used for normal LABOCA observations. Sources that are larger than the field of view (FoV) of LABOCA (about 11') can be mapped by combining maps obtained in this mode in a larger mosaic.

4.5.2 Point Suorces

Mapping is not an efficient observing mode for point sources and we defined a multiple on-off mode, called *N-on*. In this mode the source is observed sequentially by a small subset of bolometers selected for their good sensitivity, staring at the source while modulating the polarization with the polarimeter.

4.6 Data reduction

Most of the reduction of polarization data is done using the program CRUSH-2 (Comprehensive Reduction Utility for SHARC-II, A. Kovács 2008[12]) that since version 1.99a has been upgraded by A. Kovács to handle our polarization data. The program reduces the raw data and produces four FITS tables per observation, respectively containing maps of Stokes I, Q, U and the total polarization $P = \sqrt{Q^2 + U^2}$. During 2011 runs we also used BoA (the data reduction package developed for LABOCA) to reduce polarization data using new procedures developed by F. Schuller (see also contribution 8452-65 by F. Schuller to this conference). Additionally, new software written in Fortran and using the GILDAS[13] package has been developed by H. Wiesemeyer.

5. RESULTS

During the last commissioning, besides technical observations, we also did deep integrations on a small number of relevant scientific targets.The scientific outcome is still under evaluation at the moment of this writing. We observed the Moon, mainly for calibration purposes. Other calibrations have been done on Mars, Jupiter, Uranus, Neptune and some of the secondary calibrators regularly used while observing with LABOCA. We observed the extragalactic unresolved sources J1229+021 and PKS0537-441 in N-on observing mode. For this observing mode the data reduction software is still at an early stage and reduction of N-on data is still ongoing. In mapping mode we observed a few extended galactic sources (the supernova remnant NGC 1952, the molecular clouds Vela, OMC-1, OMC-3, W49, NGC 2071 and the massive YSO B13134) and the resolved nearby galaxy NGC 5128 (a.k.a. Centaurus A). Preliminary results look very promising.

5.1 The Moon

Observations of the Moon can be of great help in the process of calibrating the observed polarization position angle (PPA). The radiation emitted by regions close to the limb of the Moon, in fact, is weakly linearly polarized (see Appendix A.) The linear polarization is aligned along the radial direction while the polarization degree rapidly decreases when going from the limb to the center of the Moon. The total flux observed from the Moon is very high therefore even very small levels of polarization can be well detected in relatively short integrations. We observed the limb of the Moon in a stare-and-integrate mode (see Fig. 5) pointing the center beam of the LABOCA array at 8 fixed positions along to the limb of the Moon, integrating for 20 seconds in each position while modulating in polarization. During each integration only part of the array is actually observing the Moon, while the remaining bolometers are looking at the blank sky.

5.2 Mapping

We show here the preliminary data reduction of a large map of the supernova remnant NGC 1952 (a.k.a. Crab nebula, see Fig. 6). The polarization map spans over an area of about 6x6 arcminutes (for a comparison, see Fig. 24 in Matthews et al. 2009[14], a map of the same source done with the SCUPol[15] polarimeter.) This map combines 35 observations in compact raster of spirals mode, for a total integration time of about 90 minutes.

6. CONCLUSIONS

The installation of PolKa at the HHT in 2002 (Sect. 3.1) demonstrated that our concept of a polarimeter with a RHWP is successful. The instrument showed good polarization mapping capability, giving results of the same quality of comparable instruments (e.g. HERTZ[16], SCUPol[15], SHARP[17]).

The installation of PolKa at APEX to work in combination with LABOCA has shown to be about 50 times faster than its HHT predecessor. Moreover, it produces simultaneous maps of the first three Stokes parameters I, Q, U.

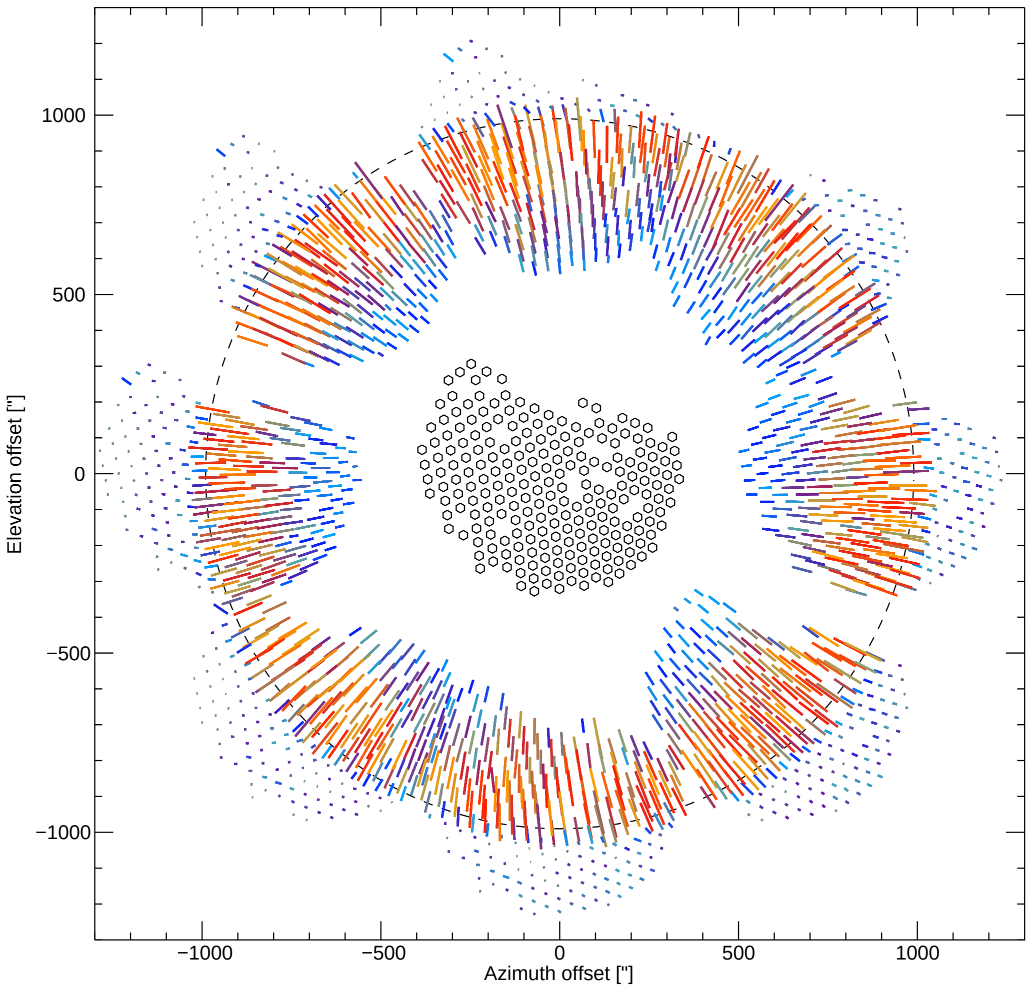

Figure 5. Observations in stare-and-integrate mode on 8 positions separated by 45 degrees along the limb of the Moon. The plot shows one polarization vector per bolometer. Color and length of each vector indicate the level of polarization measured in that position. The linear polarization is aligned along the radial direction and the intensity decreases when going from the limb to the center of the Moon. The dashed line shows the apparent size of the Moon at the time of the observations. For reference, the footprint of the array on sky at the moment of the 8 observations is shown at the center.

We are planning to complete soon the commissioning of PolKa at APEX as MPIfR PI instrument. However, some work still needs to be done before the instrument can start routine science observations. Apart from minor technical work on the hardware, we need to improve the characterization of the spurious polarization and of the spurious modulation of the total power, define a reliable calibration scheme, measure the NEFD corresponding to I and P in both mapping and N-on modes, provide a unique online data reduction pipeline.

ACKNOWLEDGMENTS

The authors would like to thank the staff at the APEX telescope for their support during the installation and on-sky testing of the instrument. Special thanks to Stefan Risse and his precision systems group at IOF, Jena.

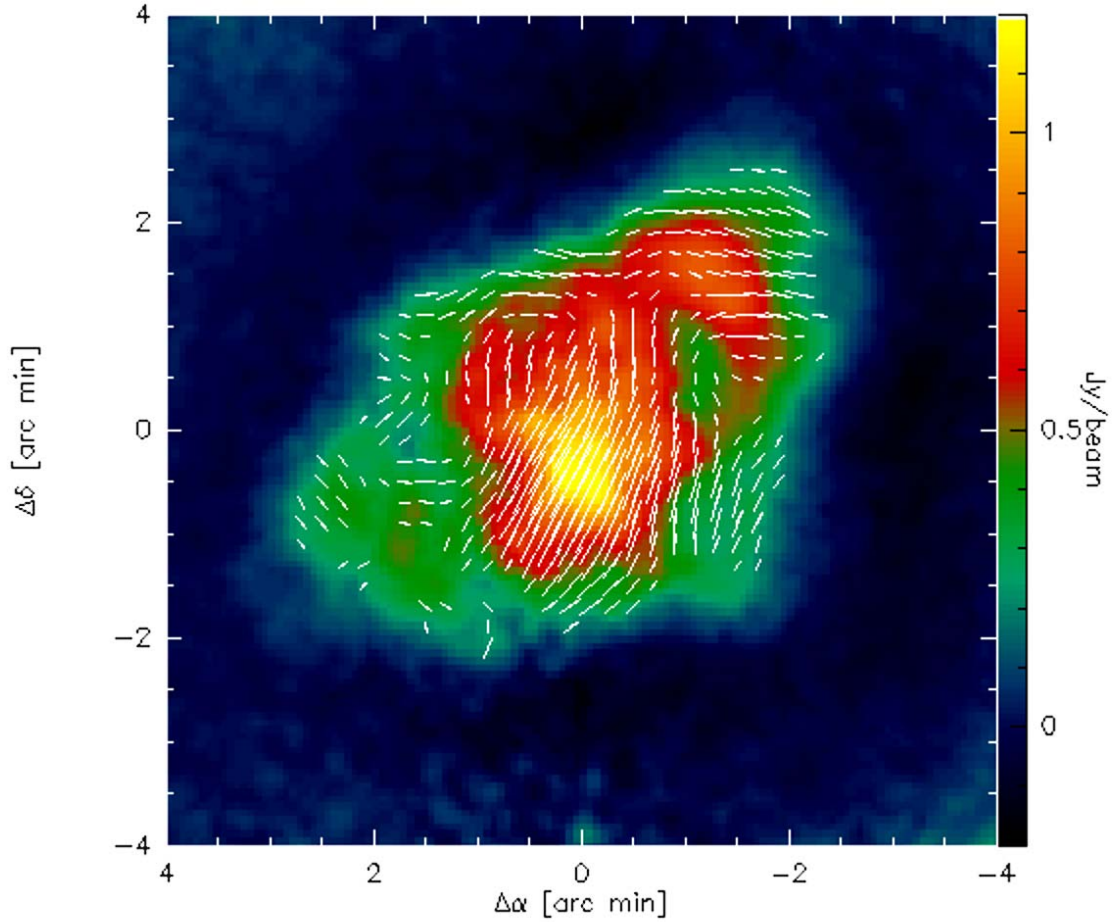

Figure 6. Map of NGC 1952 (the Crab Nebula) obtained combining 35 maps in raster of spirals observing mode for a total of 90 minutes of integration time. The color map is the total power emission observed by LABOCA. The polarization map is about 6'x6' large. The polarization vectors have been selected limiting the minimum signal-to-noise to 2.5 sigma. This map has a resolution in polarization of one vector per beam.

APPENDIX A. POLARIZATION OF THE MOON

The larger part of the mm/submm radiation that we observe as emitted by the Moon originates in a thin layer of the Moon's surface with a depth of several wavelengths. When the radiation passes from the inside of the Moon to the outside vacuum space, it is refracted following Snells law: $\epsilon_i \sin\theta_i = \epsilon_t \sin\theta_t$, where θ_i, θ_t are respectively the angle of incidence of the wave reaching the surface of the Moon from the inside and the angle of refraction of the wave transmitted to the outside. ϵ_i is the dielectric constant of the Moon's surface, in the approximation that the emitting layer has a uniform composition, and ϵ_t is the dielectric constant of space (equal to 1).

The transmission coefficients of the two components of the linear polarization, respectively in and out of the plane of incidence, are given by the Fresnel equations:

$$t_\parallel = \frac{2\epsilon_i \cos\theta_i}{\epsilon_i \cos\theta_t + \epsilon_t \cos\theta_i},\ t_\perp = \frac{2\epsilon_i \cos\theta_i}{\epsilon_i \cos\theta_i + \epsilon_t \cos\theta_t} \tag{7}$$

In general, $t_\parallel > t_\perp$, with the net result that the transmitted radiation is partially linearly polarized in the plane of incidence. The intensity of the linear polarization that we measure when observing the Moon is therefore given by

$$I_\parallel = \frac{\epsilon_t \cos\theta_t}{\epsilon_i \cos\theta_i}\ \left(t_\parallel - t_\perp\right)^2 \tag{8}$$

The first factor in Eq. 8 is due to the difference in size between the incident and transmitted area elements (ratio of cosines) and the difference in the speed of wave propagation between the moon and the space around it (ratio of dielectric constants). In the approximation that the Moon is a smooth sphere, θ_i is simply proportional to the distance of the observed point on the moon from the center of the Moon's apparent disc. Points at the center of the disc have $\theta_i = 0$ while points at the edge of the moon have $\theta_i = 90$. In this approximation, $I_\parallel$ is therefore a monotonic function of the radial distance on the Moon. Moreover, the plane of incidence for all points passes through the center of the Moon, making the net linear polarization from any point on the Moon aligned along the radial direction.

REFERENCES

[1] Cawthorne, T. V. and Wardle, J. F. C. and Roberts, D. H. and Gabuzda, D. C., "Milliarcsecond Polarization Structure of 24 Objects from the Pearson-Readhead Sample of Bright Extragalactic Radio Sources. II. Discussion," ApJ **416**, 519–+ (oct 1993).

[2] Hildebrand, R. H., "Magnetic fields and stardust," QJRAS **29**, 327–351 (Sept. 1988).

[3] Siringo, G., Kreysa, E., Kovács, A., Schuller, F., Weiß, A., Esch, W., Gemünd, H., Jethava, N., Lundershausen, G., Colin, A., Güsten, R., Menten, K. M., Beelen, A., Bertoldi, F., Beeman, J. W., and Haller, E. E., "The Large APEX BOlometer CAmera LABOCA," A&A **497**, 945–962 (Apr. 2009).

[4] Güsten, R., Nyman, L. Å., Schilke, P., Menten, K., Cesarsky, C., and Booth, R., "The Atacama Pathfinder EXperiment (APEX) - a new submillimeter facility for southern skies -," A&A **454**, L13–L16 (Aug. 2006).

[5] Siringo, G., *PolKa: a polarimeter for submillimeter bolometer arrays*, PhD thesis, Rheinische Friedrich-Wilhelms-Universität Bonn (2003).

[6] Siringo, G., Kreysa, E., Reichertz, L. A., and Menten, K. M., "A new polarimeter for (sub)millimeter bolometer arrays," A&A **422**, 751–760 (Aug. 2004).

[7] Collett, E., [*Polarized light: fundamentals and applications*], Marcel Dekker, Inc., New York (1993).

[8] Baars, J. W. M. and Martin, R. M., "The Submillimeter Telescope (SMT)," in [*Liege International Astrophysical Colloquia*], B. Kaldeich, ed., *Liege International Astrophysical Colloquia* **29**, 293–297 (Dec. 1990).

[9] Baars, J. W. M., Hooghoudt, B. G., Mezger, P. G., and de Jonge, M. J., "The IRAM 30-m millimeter radio telescope on Pico Veleta, Spain," A&A **175**, 319–326 (Mar. 1987).

[10] Kreysa, E., Gemünd, H.-P., Raccanelli, A., Reichertz, L. A., and Siringo, G., "Bolometer arrays for Mm/Submm astronomy," in [*Experimental Cosmology at Millimetre Wavelengths*], de Petris, M. and Gervasi, M., eds., *American Institute of Physics Conference Series* **616**, 262–269 (May 2002).

[11] Muders, D., Hafok, H., Wyrowski, F., Polehampton, E., Belloche, A., König, C., Schaaf, R., Schuller, F., Hatchell, J., and van der Tak, F., "APECS - the Atacama pathfinder experiment control system," A&A **454**, L25–L28 (Aug. 2006).

[12] Kovács, A., "CRUSH: fast and scalable data reduction for imaging arrays," in [*Society of Photo-Optical Instrumentation Engineers (SPIE) Conference Series*], *Society of Photo-Optical Instrumentation Engineers (SPIE) Conference Series* **7020** (Aug. 2008).

[13] IRAM, [*http://www.iram.fr/IRAMFR/GILDAS*].

[14] Matthews, B. C., McPhee, C. A., Fissel, L. M., and Curran, R. L., "The legacy of scupol: 850 m imaging polarimetry from 1997 to 2005," ApJ **182**(1), 143 (2009).

[15] Greaves, J. S., Holland, W. S., Jenness, T., Chrysostomou, A., Berry, D. S., Murray, A. G., Tamura, M., Robson, E. I., Ade, P. A. R., Nartallo, R., Stevens, J. A., Momose, M., Morino, J.-I., Moriarty-Schieven, G., Gannaway, F., and Haynes, C. V., "A submillimetre imaging polarimeter at the James Clerk Maxwell Telescope," MNRAS **340**, 353–361 (Apr. 2003).

[16] Schleuning, D. A., Dowell, C. D., Hildebrand, R. H., Platt, S. R., and Novak, G., "HERTZ, A Submillimeter Polarimeter," PASP **109**, 307–318 (Mar. 1997).

[17] Li, H., Dowell, C. D., Kirby, L., Novak, G., and Vaillancourt, J. E., "Design and initial performance of SHARP, a polarimeter for the SHARC-II camera at the Caltech Submillimeter Observatory," Appl. Opt. **47**, 422–430 (Jan. 2008).